Protein Kinase C Regulation of Intracellular and Cell Surface Amyloid Precursor Protein (APP) Cleavage in CHO695 Cells[†]

Camille Jolly-Tornetta and Bryan A. Wolf*

Department of Pathology and Laboratory Medicine, University of Pennsylvania School of Medicine, Philadelphia, Pennsylvania 19104

Received July 25, 2000

ABSTRACT: Cleavage of amyloid precursor protein (APP) by β-secretase generates β-amyloid (Aβ), the major component of senile plaques in Alzheimer's disease. Cleavage of APP by α-secretase prevents Aβ formation, producing nonamyloidogenic secreted APPs products. PKC-regulated APP α-secretase cleavage has been shown to involve tumor necrosis factor α (TNF-α) converting enzyme (TACE). To determine the location of APP cleavage, we examined PKC-regulated APPs secretion by examining cell surface versus intracellular APP in CHO cells stably expressing APP_{695} (CHO695). We demonstrate that PKC regulates cell surface and intracellular APP cleavage. The majority of secreted APPs originates from the intracellular compartment, and PKC does not cause an increase in APP trafficking to the cell surface for cleavage. Therefore, intracellular APP regulated by PKC must be cleaved at an intracellular site. Experiments utilizing Brefeldin A suggest APP cleavage occurs at the Golgi or late in the secretory pathway. Experiments using TAPI, an inhibitor of TACE, demonstrate PKC-regulated APPs secretion from the cell surface is inhibited after pretreatment with TAPI, and APPs secretion from the intracellular pool is partially inhibited after pretreatment with TAPI. These findings suggest PKC-regulated APP cleavage occurs at multiple locations within the cell and both events appear to involve TACE.

The amyloid precursor protein (APP)[1] can be processed through various pathways to generate both amyloidogenic and nonamyloidogenic peptides. APP cleavage by a β-secretase or through the endosomal or lysosomal pathway generates β-amyloid (Aβ) [reviewed in (*1, 2*)]. Recently, BACE, β-site APP-cleaving enzyme, was cloned and characterized as having β-secretase activity (*3, 4*−*6*). The β-amyloid protein is 39−43 amino acids in length and the major component of senile plaques in Alzheimer's disease (*1, 7, 8, 9*). APP processed by a constitutive secretory pathway (or α-secretase) precludes Aβ formation, producing a large secreted form ($APPs_\alpha$) and nonamyloidogenic carboxy-terminal fragments (*10, 11*). APP is a family of transmembrane glycoproteins with a large extracytoplasmic domain, a membrane-spanning domain containing the Aβ peptide, and a short intracytoplasmic domain (*12*). APP is transcribed as three alternatively spliced isoforms, ranging from 695 to 770 amino acids in length, and is expressed in mammalian neuronal and nonneuronal cells and tissues (*13*). APP gene mutations result in the aberrant processing of APP, which may lead to the deposition and accumulation of Aβ (*14, 15*−*18*). Additionally, a mutant APP transgenic mouse has been shown to express high levels of APP and Aβ in an age-dependent manner (*19*). This supports the hypothesis of a primary role for APP and Aβ in the pathogenesis of Alzheimer's disease.

Receptor-mediated regulation of $APPs_\alpha$, through muscarinic and metabotropic glutamate receptors, has been shown to involve protein kinase C (PKC) in the secretion of APPs (*20, 21*−*24*). PKC is a family of serine/threonine kinases involved in various functions in many different cells (*10, 11, 21, 25*). PKC has been shown to favor α-secretase cleavage of APP, thereby precluding the formation of Aβ, and actually decreasing Aβ generation (*26, 27*). For possible therapeutic purposes, it is important to determine how PKC is involved in the regulation of APP. PKC phosphorylates various proteins in vivo; however, it has been shown that PKC does not directly phosphorylate APP (*28, 29*). Therefore, PKC is involved in the regulation of APP through another action. One possibility is that PKC alters the trafficking of APP, and another is that PKC affects the activity of an α-secretase. Recently, tumor necrosis factor α (TNF-α) converting enzyme (TACE), also known as ADAM-17, and ADAM-10 (*a d*isintegrin *a*nd *m*etalloprotease) were implicated in PKC-regulated α-secretase cleavage of APP (*30, 31*). TACE cleaves the membrane-bound TNF-α precursor to release soluble TNF-α from cells. An inhibitor

[†] Supported by National Institutes of Health Grants AG09215 and AG11542.

* Address correspondence to this author at the Department of Pathology and Laboratory Medicine, University of Pennsylvania School of Medicine, 230 John Morgan Building, 3620 Hamilton Walk, Philadelphia, PA 19104-6082. E-mail: wolfb@mail.med.upenn.edu; Tel: 215-898-0025; FAX: 215-573-2266.

[1] Abbreviations: APP, amyloid precursor protein; Aβ, β-amyloid; ADAM, a disintegrin and metalloprotease; BACE, β-site APP-cleaving enzyme; BFA, Brefeldin A; CHO, Chinese hamster ovary; DAG, diacylglycerol; ER, endoplasmic reticulum; FITC, fluorescein isothiocyanate; IL-6Rα, interleukin-6 receptor α; PMA, phorbol 12-myristate 13-acetate; PBS, phosphate-buffered saline; PKC, protein kinase C; PS, phosphatidylserine; TGF-α, transforming growth factor α; TNF-α, tumor necrosis factor α; TACE, tumor necrosis factor α-converting enzyme; TAPI, TNF-α protease inhibitor.

10.1021/bi001723y CCC: $19.00
Published on Web 11/10/2000

of TACE has been shown to inhibit basal and PMA-induced ectodomain shedding of APP, as well as TGF-α and IL-6Rα shedding (*32*). Additionally, another inhibitor of TACE has been shown to inhibit APPs secretion, and TACE knockout mice lack the ability to induce APPs secretion with the PKC activator PMA (phorbol 12-myristate 13-acetate) (*30*). Overexpression of ADAM-10 results in an increase in PKC-stimulated APPs secretion in HEK293 cells, and expression of a dominant-negative form of ADAM-10 inhibited endogenous α-secretase activity (*31*). These current studies demonstrate a PKC-regulated α-secretase activity by the ADAM family of metalloproteases.

In addition, the location of these secretases and cleavage events has led to multiple conclusions. α-Cleavage of APP has been shown to occur at the plasma membrane, as well as in caveolae within the plasma membrane, and mature APP has been found in Golgi secretory vesicles (*33*, *34*−*37*). *β*- and *γ*-secretase activities have been described in the trans-Golgi network, in the endoplasmic reticulum/intermediate compartment, and in endosomes and lysosomes (*34*, *37*−*44*). The present study sought to investigate the location(s) of PKC-regulated APP α-cleavage by examining the source of PMA-induced APPs secretion, i.e., plasma membrane versus intracellular APP, in CHO cells stably expressing APP695 (CHO695), and the involvement of TACE/ADAM-17 activity in these cleavage events.

EXPERIMENTAL PROCEDURES

Materials. The media and serum used to maintain the CHO695 cell culture were from Gibco Co. (Grand Island, NY). The sulfo-NS-biotin and NeutrAvidin beads were from Pierce (Rockford, IL), and the phorbol esters PMA4*β* and PMA4α were from Biomol (Plymouth Meeting, PA). [^{35}S]-Methionine (1000−1500 Ci/mmol) was purchased from ICN Biomedicals (Costa Mesa, CA). The TACE inhibitor TAPI was from Peptides International (Louisville, KY).

Cell Culture of CHO695 Cells. CHO cells stably expressing APP695 were kindly provided by Dr. Virginia Lee (University of Pennsylvania). CHO695 cells were maintained in αMEM supplemented with 10% fetal bovine serum, 1% penicillin/streptomycin, and 1% L-glutamine.

Pharmacological Treatment of CHO695 Cells. CHO695 6-well plates were washed 3 times in Krebs−Hepes buffer (25 mM Hepes, pH 7.4, 115 mM NaCl, 24 mM $NaHCO_3$, 5 mM KCl, 2.5 mM $CaCl_2$, 1 mM $MgCl_2$, 0.1% bovine serum albumin, 3 mM D-glucose), and then incubated under an atmosphere of 95% O_2/5% CO_2 at 37 °C for the appropriate time with PMA. To examine the effect of Brefeldin A or nocodazole, the cells were pretreated with the agents for the appropriate time at 37 °C and then incubated for an additional 60 min alone or in the presence of PMA. To examine the effect of the TACE inhibitor, TAPI, the cells were pretreated for 30 min with TAPI, and then incubated for an additional 60 min alone or in the presence of PMA.

Biotinylation of CHO695 Cells (Detection by [^{35}S]Methionine Labeling, Figure 1). CHO695 cells grown in 6-well plates were serum-starved for 20 min in DMEM methionine-free media and then labeled with 500 μCi/mL [^{35}S]methionine in DMEM methionine-free media (1% penicillin/streptomycin, 5% fetal bovine serum) for 3 h at 37 °C. The cells were then washed twice in phosphate-buffered saline (PBS), and 0.5 mg/mL of sulfo-NS-biotin was added for 30 min at 4 °C. After biotinylation, the cells were washed again in PBS, and treated with and without 10 μM PMA for 60 min at 37 °C. After treatment, the supernatant (media) was removed and centrifuged for 15 min at 15000*g* to remove any remaining cells. NeutrAvidin beads were added to the supernatants, and the next day the samples were centrifuged and the supernatants transferred to new tubes containing protein A−Sepharose beads preabsorbed to rabbit α-goat IgG. The supernatant containing the remaining nonbiotinylated APP was immunoprecipitated with 1−2 μg of an anti-APP polyclonal antibody (Karen) as previously described (*45*). The NeutrAvidin beads were washed, and sample buffer (15 mg/mL DTT) was added. Immunoprecipitates (with equivalent protein levels) were analyzed on 7.5% SDS−PAGE mini-gels, and the radioactivity was quantitated using Image Quant software on a Molecular Dynamics PhosphorImager. For data analysis, the control was designated as 100% within each experiment due to the differences in radioactive counts between the controls in separate experiments.

Biotinylation of CHO695 Cells (Detection by Western Blotting). CHO695 cells were biotinylated and treated with PMA as described above, and the samples were processed as described above. After analyzing samples (with equivalent protein levels) on 7.5% SDS−PAGE mini-gels, proteins were then transferred to nitrocellulose paper (Hybond C; Amersham) at 100 V for 2 h. The nitrocellulose paper was blocked overnight (1% bovine serum albumin, 10 mM Tris, pH 7.40, 150 mM NaCl, and 0.1% sodium azide), and the next day the blots were probed with a specific goat polyclonal anti-APP antibody (Karen). The blots were washed twice with 10 mM Tris, pH 7.40, 150 mM NaCl, and 0.1% sodium azide (TNA) for 10 min, once with TNA supplemented with 0.05% Nonidet P-40 for 5 min, and twice more with TNA for 10 min. The blots were then incubated for 1 h at room temperature with a rabbit anti-goat antibody. The blots were washed with TNA as before, the proteins detected with [^{125}I]-Protein A, and the blots washed as described. Proteins were visualized using Image Quant software on a Molecular Dynamics PhosphorImager.

Trafficking of APP. CHO695 6-well plates were treated with and without PMA for various times, and then washed with PBS. The cells were then biotinylated with sulfo-NS-biotin for 30 min at 4 °C. The cells were again washed with PBS, and lysed in 50 mM Tris base (pH 8.0), 150 mM NaCl, 1% NP40, 5 mM EDTA (+ protease inhibitors). Samples were centrifuged, and the supernatant was transferred to tubes containing NeutrAvidin beads. The next day the beads were washed and sample buffer (+15 mg/mL DTT) was added. The samples were analyzed on a 7.5% SDS−PAGE mini-gel, and the proteins were transferred to nitrocellulose membranes. The membranes were blotted with an anti-APP antibody and probed with [^{125}I]Protein A. Proteins were visualized and quantitated using Image Quant software on a Molecular Dynamics PhosphorImager.

Data Analysis. Results were analyzed by two-way ANOVA, or one-way analysis of variance was used, followed by the Bonferroni post-test. Differences were considered significant for $p < 0.05$.

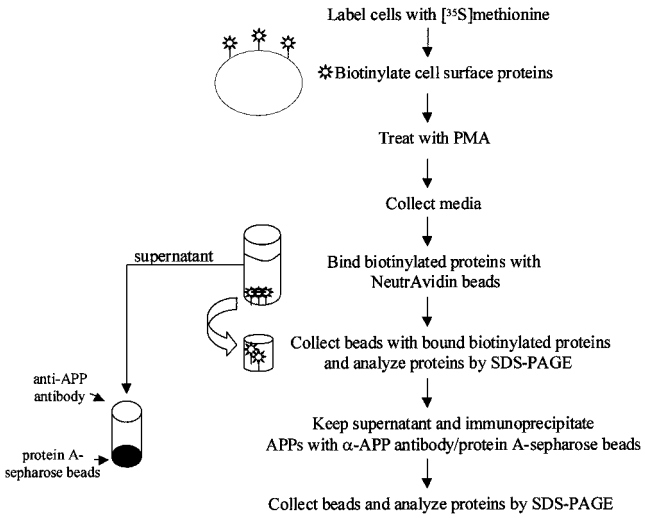

FIGURE 1: Schematic of biotinylation method.

RESULTS

Validation of the Biotinylation Method. Preliminary studies were performed to validate the biotinylation protocol (Figure 1). In brief, CHO695 cells were biotinylated with various concentrations of cell-impermeable sulfo-NHS-biotin to determine the optimal biotin concentration and identify the saturation point of the biotin. Our results demonstrate that increasing the biotin above 0.5 mg/mL did not increase the amount of recoverable biotinylated APP, suggesting that the biotinylation is complete. Different amounts of NeutrAvidin beads were also tested in order to determine the optimal concentration of beads for maximum binding to biotin. In addition, after biotinylation of the cells, the supernatants collected were subjected to successive NeutrAvidin bead incubations to ensure that the beads were able to bind all biotinylated APP during the first incubation. We determined that 30 μL of the NeutrAvidin beads was sufficient to bind all the biotinylated APP during the first incubation and adding more than 30 μL did not increase the recovery of the biotinylated proteins. Immunofluorescence was also performed using streptavidin bound to fluorescein isothiocyanate (FITC), verifying that the biotin was cell impermeable and that there was cell surface biotinylation.

Preliminary experiments were also performed to validate the immunoprecipitation of APP. In brief, CHO695 cells were metabolically labeled with [^{35}S]methionine and then treated with PMA. The medium was collected and an anti-APP antibody added. Various concentrations of protein A−Sepharose beads, preabsorbed to rabbit anti-goat IgG, were then added to determine the optimal amount needed for complete binding. In addition, the medium was subjected to successive immunoprecipitations with the anti-APP antibody and the protein A−Sepharose to ensure that all of the available APP was bound. We found that 35 μL of the protein A−Sepharose was sufficient to bind all the APP during the first immunoprecipitation.

PMA Causes an Increase in APPs Secretion from the Cell Surface and from the Intracellular Compartment. Experimentally, CHO695 cells were metabolically labeled with [^{35}S]methionine, biotinylated, and then treated with PMA for 60 min. The secreted biotinylated proteins were detected by binding to NeutrAvidin beads, and the nonbiotinylated APP was detected by subsequent immunoprecipitation with an anti-APP antibody. Figure 2A demonstrates that PMA causes a 2.6-fold increase in biotinylated APP (i.e., APP from the cell surface), and Figure 2B shows a 3.6- and 3.9-fold increase in total APPs secretion and APPs secretion from the intracellular compartment, respectively ($p < 0.001$ versus control). The amount of APPs remaining after the biotinylated APPs was removed is equivalent to the amount of total APPs secreted, suggesting that the majority of the PMA-induced APP secretion is coming from the intracellular compartment and only a small fraction from the cell surface. Table 1 also demonstrates that PMA causes the release of APP from the cell surface into the media and also an increase in APPs secretion from the intracellular compartment. In addition, the mature intracellular APP is dramatically reduced after PMA treatment, and the immature intracellular APP is unaffected, suggesting that the mature APP is cleaved and then released. Table 1 also shows that the majority of the APP is located within the intracellular compartment (~91%) and that APP on the cell surface accounts for only a small percentage (~9%) of the total APP.

Table 1: Distribution of APP in CHO695 Cells[a]

	control (vehicle)	PMA
secreted APP (from cell surface)	93000[b] (=100%)	530000[b] (570%)
secreted APP (from intracellular compartment)	300000[b] (=100%)	1300000[b] (428%)
intracellular APP		
mature	260000[b] (=100%)	47000[b] (18%)
immature	340000[b] (=100%)	330000[b] (96%)

[a] Cells were labeled for 3 h with [^{35}S]methionine as in Figure 2, treated with and without NHS-sulfo-biotin, and then treated with vehicle (control) or 10 μM PMA for 60 min. APPs secreted from the cell surface was determined after binding with NeutrAvidin beads, and the APP secreted from the intracellular compartment was determined after subsequent immunoprecipitation with an anti-APP antibody. Intracellular APP, mature and immature, was determined by immunoprecipitation with the anti-APP antibody. [b] Cellular APP and secreted APP were quantitated by PhosphorImager analysis as the amount of radioactivity in the APP band and are expressed as the average of the amount of the radioactivity (arbitrary units) and as a percentage of the control within each experiment. Results are from 4 separate observations/condition.

The Majority of PMA-Induced APPs Secretion Comes from the Intracellular Compartment. To substantiate the findings in Figure 2 that the majority of the PMA-induced APPs secretion is coming from an intracellular compartment, trypsin was used to cleave cell surface proteins, i.e., APP. The removal of cell surface APP would allow for the examination of PMA-regulated APP from the intracellular compartment only. CHO695 cells were metabolically labeled with [^{35}S]methionine, biotinylated, trypsinized, and then treated with PMA for 60 min. Figure 3A demonstrates the effectiveness of the trypsin treatment on secreted biotinylated proteins as detected with NeutrAvidin beads. Figure 3B demonstrates that PMA causes a 3.6- and 5.2-fold increase in total APPs secretion and APPs secretion from the intracellular compartment, respectively ($p < 0.0001$ versus control). The amount of APPs remaining after the removal of cell surface proteins by trypsin treatment is equivalent to the amount of total APPs secreted, suggesting again that the majority of the PMA-regulated APPs secretion is coming from an intracellular compartment.

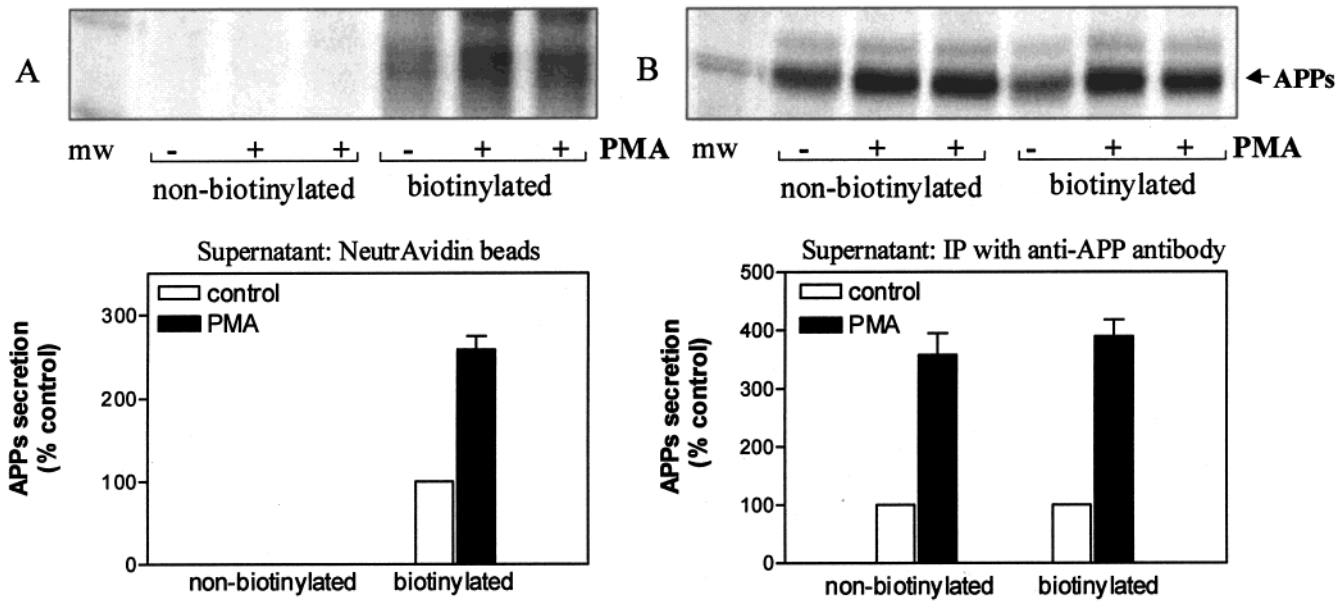

FIGURE 2: Effect of phorbol ester PMA on APPs secretion from the cell surface and from the intracellular compartment in CHO695 cells. CHO695 cells were labeled for 3 h with [^{35}S]methionine, treated with or without sulfo-NHS-biotin for 30 min, and then treated for 60 min with the vehicle (control) or 10 μM PMA. The supernatant (media) was removed, and NeutrAvidin beads were added to bind the biotinylated proteins. After binding, the supernatants were transferred to new tubes containing protein A−Sepharose beads preabsorbed to rabbit α-goat IgG, and the remaining nonbiotinylated APP was immunoprecipitated with an anti-APP polyclonal antibody. Top panel A: Representative gel showing the biotinylated (cell surface) APPs band after precipitation with NeutrAvidin beads. Top panel B: Representative gel showing the remaining nonbiotinylated (intracellular) 110 kDa APPs band after precipitation with NeutrAvidin beads and subsequent immunoprecipitation with an anti-APP antibody. Bottom panels: APPs secretion, cell surface and intracellular compartment, after treatment with PMA. APPs secretion was quantitated by a PhosphorImager as the amount of radioactivity in the APPs band and is expressed as a percentage of the control within each experiment. Results are shown as the mean ± SE of APPs secretion from 6−12 separate observations/condition.

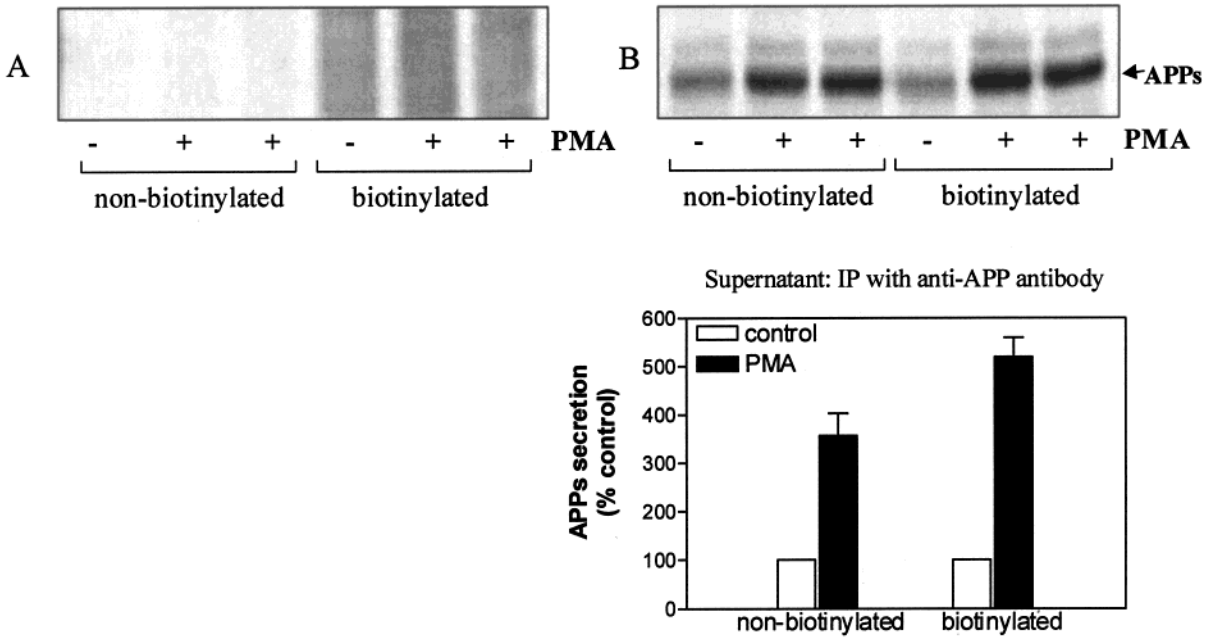

FIGURE 3: Effect of trypsin on PMA-induced APPs secretion from the cell surface and from the intracellular compartment in CHO695 cells. CHO695 cells were labeled for 3 h with [^{35}S]methionine, treated for 30 min with or without sulfo-NHS-biotin, treated with 10 μg/mL trypsin for 30 min at 4 °C, and then treated for 60 min with the vehicle (control) or 10 μM PMA. The supernatant (media) was removed, and NeutrAvidin beads were added to bind the biotinylated proteins. After binding, the supernatants were transferred to new tubes containing protein A−Sepharose beads preabsorbed to rabbit α-goat IgG, and the remaining nonbiotinylated APP was immunoprecipitated with an anti-APP polyclonal antibody. Top panel A: Representative gel showing the biotinylated (cell surface) APPs band after precipitation with NeutrAvidin beads. Top panel B: Representative gel showing the remaining nonbiotinylated (intracellular) 110 kDa APPs band after precipitation with NeutrAvidin beads and subsequent immunoprecipitation with an anti-APP antibody. Bottom panel. APPs secretion, intracellular compartment, after treatment with trypsin and with PMA. APPs secretion was quantitated by a PhosphorImager as the amount of radioactivity in the APPs band and is expressed as a percentage of the control within each experiment. Results are shown as the mean ± SE of APPs secretion from 2−4 separate observations/condition.

PMA Causes an Increase in APPs Secretion from the Cell Surface and from the Intracellular Compartment As Shown by Western Blotting. To verify that the biotinylated proteins seen in Figure 2 were in fact APP, the experiment was

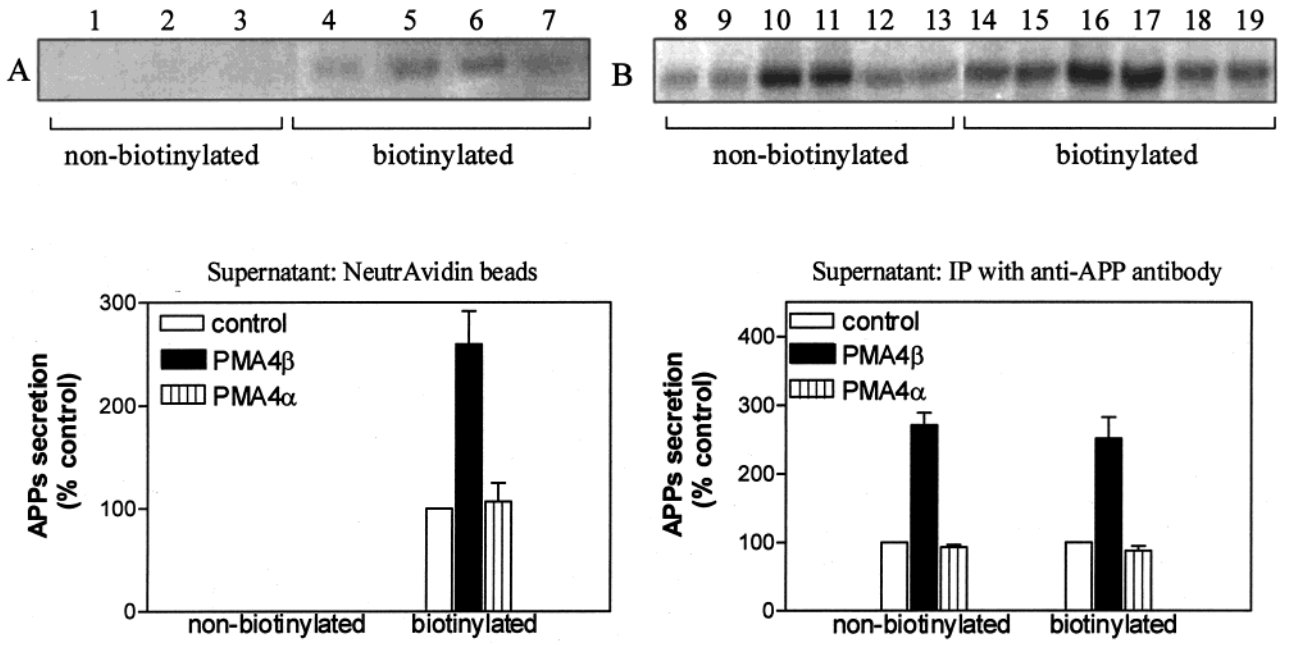

FIGURE 4: Effect of phorbol ester PMA on APPs secretion from the cell surface and from the intracellular compartment in CHO695 cells. CHO695 cells were treated for 30 min with or without sulfo-NHS-biotin, and then treated for 60 min with the vehicle (control) (lanes 1, 4, 8, 9, 14, 15), 10 μM PMA4β (active) (lanes 2, 3, 5, 6, 10, 11, 16, 17), or PMA4α (inactive analogue) (lanes 7, 12, 13, 18, 19). The supernatant (media) was removed, and NeutrAvidin beads were added to bind the biotinylated proteins. After binding, the supernatants were transferred to new tubes containing protein A−Sepharose beads preabsorbed to rabbit α-goat IgG, and the remaining nonbiotinylated APP was immunoprecipitated with an anti-APP polyclonal antibody. Proteins were analyzed on SDS−PAGE mini-gels and APP proteins detected by Western blotting with an anti-APP antibody. Top panel A: Representative immunoblot showing the biotinylated (cell surface) APPs band after precipitation with NeutrAvidin beads. Top panel B: Representative immunoblot showing the remaining nonbiotinylated (intracellular) 110 kDa APPs band after precipitation with NeutrAvidin beads and subsequent immunoprecipitation with an anti-APP antibody. Bottom panels: APPs secretion, cell surface and intracellular compartment, after treatment with PMA. APPs secretion was quantitated by a PhosphorImager as the amount of radioactivity in the APPs band and is expressed as a percentage of the control within each experiment. Results are shown as the mean ± SE of APPs secretion from 2−8 separate observations/condition.

repeated using the western blotting technique and an anti-APP antibody. CHO695 cells were biotinylated and treated with PMA for 60 min. The medium was collected, and the biotinylated proteins, i.e., cell surface proteins, were detected by binding with NeutrAvidin beads. The supernatant remaining after removal of the biotinylated proteins was assayed for nonbiotinylated APP, i.e., intracellular APP, by immunoprecipitation. The samples were then analyzed by SDS−PAGE and immunoblotted with an anti-APP-specific antibody. Figure 4A shows that again PMA causes an increase in biotinylated APPs secretion (2.8-fold), and that the inactive PMA analogue, PMA4α, does not have an effect on APPs secretion. Figure 4B confirms the results found with metabolic labeling that the majority of PMA-induced APPs secretion is coming from the intracellular compartment by the fact that there is a 2.7-fold increase with PMA of total APPs secretion and a 2.5-fold increase with PMA of APPs secretion after removing the biotinylated APP, i.e., APP from the intracellular compartment.

PMA Causes the Release of Full-Length, Mature APP. CHO695 cells were metabolically labeled with [^{35}S]methionine for 3 h and treated with PMA as described above for 60 min. The medium was collected, and the cells were washed with PBS and lysed. The APP in the media and the cell lysate was immunoprecipitated with an antibody against the N-terminus of APP (Karen) or the α-cleavage site (6E10). Therefore, Karen will recognize full-length and cleaved APP, and 6E10 will recognize cleaved APP. Intracellular APP can be detected as immature APP, without all posttranslational modifications, or as fully glycosylated, mature APP. Figure 5 shows that PMA causes nearly all of the full-length, mature APP to be released from the cell and secreted into the media.

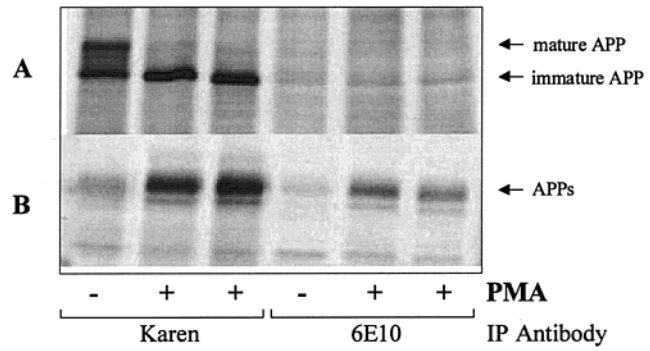

FIGURE 5: Effect of PMA on intracellular APP and secreted APP from CHO695 cells. CHO695 cells were labeled for 3 h with [^{35}S]-methionine and treated for 60 min with the vehicle (control) or 10 μM PMA. APP was immunoprecipitated with an N-terminal antibody (Karen) or an antibody that recognizes the α-cleavage site (6E10). Panel A: Representative gel showing the intracellular mature and immature APP bands after immunoprecipitation of lysates with Karen or 6E10 antibodies. Panel B: Representative gel showing the secreted APPs band after immunoprecipitation of the supernatant with Karen or 6E10. APPs secretion was quantitated by a PhosphorImager as the amount of radioactivity in the APPs band and is expressed as a percentage of the control within each experiment. Results are shown as the mean ± SE of APPs secretion from 2−4 separate observations/condition.

PMA-Induced APPs Secretion Is Inhibited by Brefeldin A. CHO695 cells were labeled with [^{35}S]methionine for 3 h in the presence or absence of 10 μg/mL Brefeldin A (BFA).

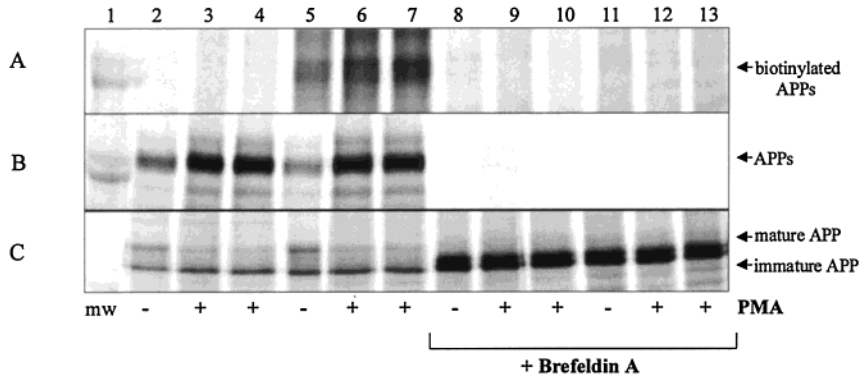

FIGURE 6: Effect of Brefeldin A on PMA-induced APPs secretion from the cell surface and APP from the intracellular compartment in CHO695 cells. CHO695 cells were labeled for 3 h with [^{35}S]methionine in the presence or absence of 10 μg/mL BFA, treated for 30 min with or without sulfo-NHS-biotin in the presence or absence of 10 μg/mL BFA, and then treated for 60 min with the vehicle (control) or 10 μM PMA in the presence or absence of 10 μg/mL BFA. The supernatant (media) was removed, and NeutrAvidin beads were added to bind the biotinylated proteins. After binding, the supernatants were transferred to new tubes containing protein A−Sepharose beads preabsorbed to rabbit α-goat IgG, and the remaining nonbiotinylated APP was immunoprecipitated with an anti-APP polyclonal antibody. Panel A: Representative gel showing the biotinylated (cell surface) APPs band after precipitation with NeutrAvidin beads. Panel B: Representative gel showing the remaining nonbiotinylated (intracellular) 110 kDa APPs band after precipitation with NeutrAvidin beads and subsequent immunoprecipitation with an anti-APP antibody. Panel C: Representative gel showing intracellular APP after immunoprecipitation with anti-APP antibody (lanes 2−4 and 8−10, not biotinylated; lanes 5−7 and 11−13, biotinylated). APPs secretion was quantitated by a PhosphorImager as the amount of radioactivity in the APPs band and is expressed as a percentage of the control within each experiment. Results are shown as the mean ± SE of APPs secretion from 2−4 separate observations/condition.

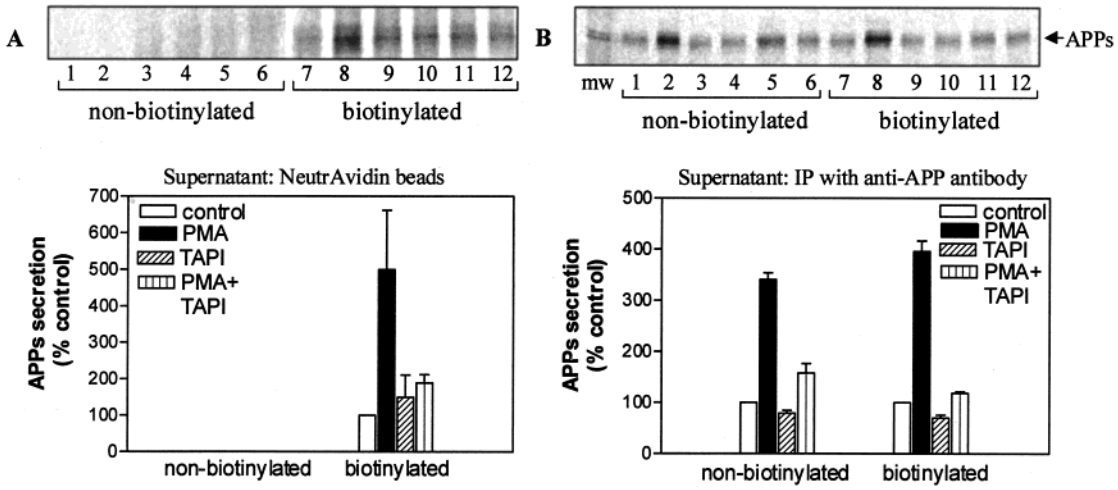

FIGURE 7: Effect of TAPI on PMA-induced APPs secretion from the cell surface and from the intracellular compartment in CHO695. CHO695 cells were labeled for 3 h with [^{35}S]methionine, treated for 30 min with or without sulfo-NHS-biotin, pretreated for 30 min with or without 20 μM TAPI, and then treated for 60 min with the vehicle (control) (lanes 1, 7), 10 μM PMA (lanes 2, 8), 20 μM TAPI (lanes 3, 4, 9, 10), or PMA + TAPI (lanes 5, 6, 11, 12). The supernatant (media) was removed, and NeutrAvidin beads were added to bind the biotinylated proteins. After binding, the supernatants were transferred to new tubes containing protein A−Sepharose beads preabsorbed to rabbit α-goat IgG, and the remaining nonbiotinylated APP was immunoprecipitated with an anti-APP polyclonal antibody. Top panel A: Representative gel showing the biotinylated (cell surface) APPs band after precipitation with NeutrAvidin beads. Top panel B: Representative gel showing the remaining nonbiotinylated (intracellular) 110 kDa APPs band after precipitation with NeutrAvidin beads and subsequent immunoprecipitation with an anti-APP antibody. Bottom panels: APPs secretion after pretreatment with TAPI and treatment with PMA ± TAPI. APPs secretion was quantitated by a PhosphorImager as the amount of radioactivity in the APPs band and is expressed as a percentage of the control within each experiment. Results are shown as the mean ± SE of APPs secretion from 2−4 separate observations/condition.

Cells were biotinylated and then treated with PMA alone or in the presence of BFA. BFA is a fungal metabolite that prevents newly synthesized proteins from exiting the ER, causes disruption of the Golgi and retrograde transport back to the ER, and inhibits transport of proteins from the Golgi to the cell surface (*46*−*50*). Figure 6A shows that BFA prevents biotinylated APPs secretion, i.e., cell surface APP release, suggesting that BFA prevents APP from sorting to the cell surface. Figure 6B shows that BFA also prevents the intracellular APP from being secreted. Figure 6C demonstrates that BFA causes the accumulation of immature forms of intracellular APP. Since BFA prevents the maturation of APP through the Golgi, APP is not able to sort to the plasma membrane or be secreted into the media. These results suggest that intracellular APP cleavage occurs later in the secretory pathway. Treatment of the cells with nocodazole, a microtubule depolymerizing agent, did not have any effect on APPs secretion from the cell surface and from the intracellular compartment (data not shown).

Inhibition of Cell Surface and Intracellular Cleavage by TAPI. CHO695 cells were labeled for 3 h with [^{35}S]-methionine, biotinylated, and then pretreated for 30 min with 20 μM TAPI. The cells were then treated with PMA alone or in the presence of TAPI. Figure 7A demonstrates the

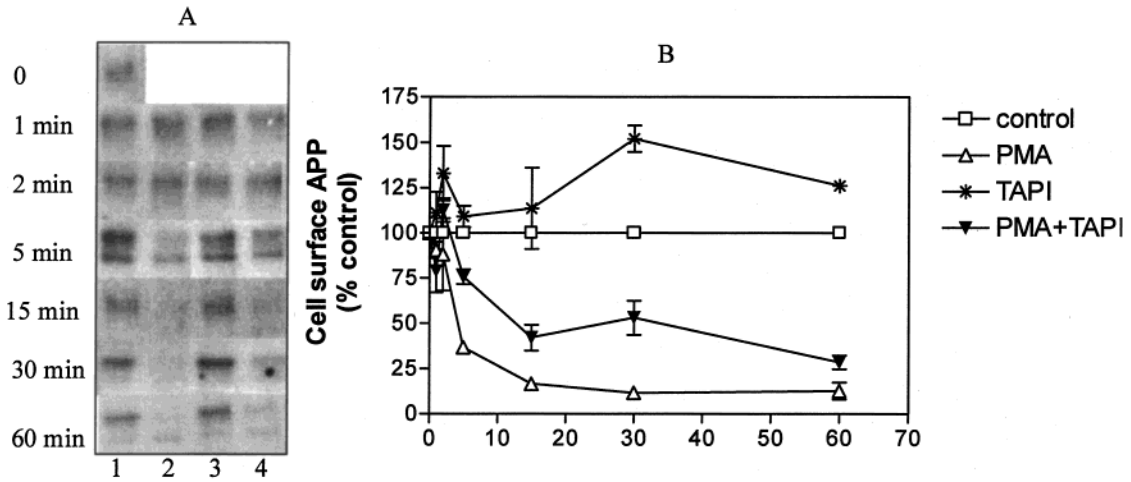

FIGURE 8: Effect of PMA on APP trafficking to the cell surface in CHO695 cells. CHO695 cells were pretreated for 30 min in the presence or absence of 20 μM TAPI, and then treated for various times with the vehicle (control) (lane 1), 10 μM PMA (lane 2), 20 μM TAPI (lane 3), or 10 μM PMA + 20 μM TAPI (lane 4). The cells were then biotinylated for 30 min with sulfo-NHS-biotin. The biotinylated cell surface proteins were detected with NeutrAvidin beads. The proteins were analyzed by SDS−PAGE mini-gels, and the cell surface APP was detected by western blotting with an anti-APP antibody. Panel A: Representative immunoblot of the effect of PMA on cell surface APP over time. Panel B: Time course of the effect of PMA on cell surface APP.

inhibition of APPs secretion from the cell surface, suggesting that TAPI inhibits cell surface APP cleavage. Figure 7B shows that TAPI also inhibits APPs secretion from the intracellular compartment, again suggesting that TAPI inhibits intracellular APP cleavage. However, PMA is still able to cause a 2-fold and 1.7-fold (Figure 7B) increase in APPs secretion in the presence of TAPI versus TAPI alone. TAPI does not seem to affect constitutive APP secretion from the intracellular compartment or the cell membrane.

Depletion of Cell Surface APP with PMA. CHO695 cells were treated with PMA for various times, and then biotinylated. After lysing the cells, the biotinylated cell surface proteins were analyzed by SDS−PAGE and immunoblotted with an anti-APP antibody. Figure 8 demonstrates a time-dependent decrease in cell surface APP with PMA. These results suggest that PMA does not cause APP trafficking to the cell surface for cleavage, therefore implying again that there is also intracellular cleavage of APP.

DISCUSSION

We have shown that PKC causes the redistribution of mature APP from an intracellular site and the cell membrane to the media of CHO695 cells. A small portion of the APPs secreted was found to be cleaved from the cell surface; however, the majority of the APPs was from the intracellular compartment, suggesting that APP cleavage occurs both inside the cell as well as at the plasma membrane. PKC-regulated cleavage at the cell surface and at an intracellular location appears to involve TACE and/or ADAM-10 due to the inhibition of the secretion of APP by TAPI, an inhibitor of TACE. Experiments utilizing agents that affect protein trafficking through the endoplasmic reticulum (ER) and Golgi suggest that intracellular cleavage of APP occurs beyond the ER after maturation and posttranslational modification of APP in the Golgi. Previous studies have demonstrated that APP mutants defective in O-glycosylation accumulate in reticular compartments such as the endoplasmic reticulum and there is a decrease in the intracellular production of C-terminal fragments and the production of Aβ in the medium (*51*). These results suggest that APP is cleaved during or after maturation (O-glycosylation) of APP after the trans-Golgi or during transport through the Golgi.

The constitutive APP secretory pathway represents a major pathway of APP degradation. This involves the cleavage of APP by an α-secretase, which releases a large secreted N-terminal fragment, and subsequent cleavage of the membrane-bound C-terminal segment by a γ-secretase produces a 3 kDa nonamyloidogenic fragment. APP α-secretase cleavage is thought to occur at Lys^{16} within the Aβ sequence; however, the cleavage appears to be determined by the cleavage site conformation and the distance from the membrane, rather than a specific sequence. APP and α-secretase activities have been localized to the Golgi, as well as post-Golgi, secretory vesicles (*36, 37, 52*). APP and APP α-secretase cleavage products have also been found in caveolae, invaginations in the plasma membrane containing caveolin, a protein that binds other proteins, cholesterol, and glycospingolipids (*35*). Conversely, the upregulation of caveolin-3 stimulates β-secretase activity in COS cells cotransfected with APP_{695} and caveolin-3 (*53*). APP, as well as other transmembrane proteins, can be cleaved at the plasma membrane, also referred to as "ectodomain shedding", and has been shown to involve a metalloprotease (*32*−*34*). APP internalized from the cell membrane is degraded in the endosomal or lysosomal pathway and can produce the amyloidogenic Aβ peptide (*34, 41, 42, 44*). APP can also be cleaved by β- and γ-secretases to generate Aβ (*17, 54, 55*). These secretase activities have been demonstrated in the trans-Golgi network, in the endoplasmic reticulum/intermediate compartment, and also in endosomes and lysosomes (*34, 37*−*44*). Most recently, an aspartic protease BACE, β-site APP-cleaving enzyme, was cloned and characterized as exhibiting β-secretase activity (*3*−*6*).

In contrast, the location of regulated APP cleavage has been studied less extensively. It is important to understand PKC-regulated APP cleavage since PKC activation results in the cleavage of APP into nonamyloidogenic peptides, and in the reduction of Aβ production (*26, 27, 56, 57*). PKC has

been extensively studied and shown to be involved in the regulation of APPs secretion (*10, 11, 21, 25*). Both muscarinic regulation and glutamatergic regulation of APPs secretion have been shown to involve PKC downstream of their receptors (*20*−*24*). However, the mechanism by which PKC results in the secretion of APP is not well understood. PKC is not involved in the direct phosphorylation of APP; therefore, it is possible that PKC activates an α-secretase or causes APP to redistribute from the Golgi to another compartment for cleavage. PKC does not appear to cause APP to redistribute from an intracellular compartment to the cell surface. We demonstrate that activation of PKC causes a time-dependent decrease in the amount of APP at the cell surface, and an increase in the appearance of APPs in the media. This suggests that PKC does not cause redistribution of APP from the Golgi to the cell surface for cleavage; therefore, in our system the majority of APP cleavage occurs within an intracellular compartment.

The ADAM family of metalloproteases was first shown to be involved in the ectodomain shedding of many cell surface transmembrane proteins, such as TNF-α, transforming growth factor α (TGF-α), other growth factors and growth factor receptors, and cell adhesion molecules (*32, 58*−*60*). Recently, TACE/ADAM-17 and ADAM-10, members of the metalloprotease family, were shown to be involved in PKC-regulated APPs secretion (*30, 31*). Disruption of the TACE gene in mouse fibroblasts inhibited the secretion of PMA-induced APPs secretion, but did not affect the constitutive production and secretion of APP (*30*). Overexpression of ADAM-10 increased both basal as well as protein kinase C-stimulated APPs secretion (*31*). Additionally, a dominant-negative ADAM-10 mutant inhibited endogenous α-secretase activity. The majority of the active form of ADAM-10 is found at the cell surface; however, the proenzyme of ADAM-10 has also been detected in the Golgi, supporting the idea that APP cleavage occurs at the cell membrane. Two glycosylphosphatidylinositol-linked aspartyl proteases, termed yapsin, have recently been identified in yeast that are active at the cell membrane and are able cleave human APP at the α-secretase cleavage site, releasing it into the media (*61*). These results suggest that different enzymes may be involved in constitutive versus PKC-regulated APPs secretion, and that possibly different α-secretases are involved in cell surface versus intracellular APP cleavage.

This study provides a novel insight into the regulation of APPs secretion by PKC. First, our results demonstrate that the majority of PKC-regulated APPs secretion is due to cleavage within an intracellular compartment, and a minority from cleavage at the cell surface. Second, the cell surface APP cleavage appears not to be just "ectodomain shedding" or constitutive cleavage, but rather regulated cleavage that involves PKC and TACE. Likewise, the PKC-regulated intracellular cleavage also appears to involve TACE, but not completely. TAPI only slightly inhibits PKC-regulated APP cleavage from the intracellular compartment. TAPI inhibits the overall amount of APP secreted, but only slightly decreases the fold of PKC-regulated secretion over the secretion with TAPI alone. This could be due to an incomplete inhibition of TACE by TAPI or due to the involvement of more than one secretase in the intracellular cleavage of APP. However, TAPI seems to completely inhibit the PMA-induced APPs secretion from the cell surface, suggesting that TAPI is effectively blocking the action of the TACE. In addition, inhibition of TACE with TAPI was able to retain APP at the cell surface even after treatment with PMA, implying that TAPI inhibited the cell surface cleavage of APP by TACE. Furthermore, the recent evidence implicating different enzymes, the metalloproteases and the aspartyl proteases, in the regulation of APPs secretion provides the basis for the involvement of multiple enzymes in the constitutive and regulated cleavage of APP. For both the intracellular and cell surface cleavage of APP, TACE does not appear to be involved in the constitutive cleavage and secretion. However, TACE does seem to be involved in the regulated cleavage of APP from the cell surface and to some extent in the intracellular cleavage of APP.

In conclusion, we have shown that PKC regulates both cell surface as well as intracellular cleavage of APP, resulting in the secretion of APPs. PKC does not cause trafficking of APP to the cell surface for cleavage, but rather is involved in the regulation of APP cleavage. The intracellular site(s) of APP cleavage occur(s) after maturation of APP in the trans-Golgi or later in the secretory pathway. TACE is not involved in the basal production and secretion of APP, but rather in the regulated cell surface cleavage of APP, and to some extent in the regulated intracellular cleavage of APP. However, the majority of the PKC-regulated APPs secretion is coming from the intracellular compartment, suggesting that PKC-regulated APP cleavage and secretion could involve more than one α-secretase.

ACKNOWLEDGMENT

We thank Patricia Jegier for her technical assistance and maintenance of the cell line. We also thank Drs. Virginia Lee, Robert Doms, and Nelson Cole for their constructive input regarding this project.

REFERENCES

1. Selkoe, D. J., Yamazaki, T., Citron, M., Podlisny, M. B., Koo, E. H., Teplow, D. B., and Haass, C. (1996) *Ann. N.Y. Acad. Sci. 777*, 57−64.
2. Selkoe, D. J. (1999) *Nature 399*, Suppl. 31.
3. Vassar, R., Bennett, B. D., Babu-Khan, S., Kahn, S., Mendiaz, E. A., Denis, P., Teplow, D. B., Ross, S., Amarante, P., Loeloff, R., Luo, Y., Fisher, S., Fuller, J., Edenson, S., Lile, J., Jarosinski, M. A., Biere, A. L., Curran, E., Burgess, T., Louis, J. C., Collins, F., Treanor, J., Rogers, G., and Citron, M. (1999) *Science 286*, 735−741.
4. Yan, R., Bienkowski, M. J., Shuck, M. E., Miao, H., Tory, M. C., Pauley, A. M., Brashier, J. R., Stratman, N. C., Mathews, W. R., Buhl, A. E., Carter, D. B., Tomasselli, A. G., Parodi, L. A., Heinrikson, R. L., and Gurney, M. E. (1999) *Nature 402*, 533−537.
5. Sinha, S., Anderson, J. P., Barbour, R., Basi, G. S., Caccavello, R., Davis, D., Doan, M., Dovey, H. F., Frigon, N., Hong, J., Jacobson-Croak, K., Jewett, N., Keim, P., Knops, J., Lieberburg, I., Power, M., Tan, H., Tatsuno, G., Tung, J., Schenk, D., Seubert, P., Suomensaari, S. M., Wang, S., Walker, D., and John, V. (1999) *Nature 402*, 537−540.
6. Hussain, I., Powell, D., Howlett, D. R., Tew, D. G., Meek, T. D., Chapman, C., Gloger, I. S., Murphy, K. E., Southan, C. D., Ryan, D. M., Smith, T. S., Simmons, D. L., Walsh, F. S., Dingwall, C., and Christie, G. (1999) *Mol. Cell. Neurosci. 14*, 419−427.
7. Hardy, J., and Allsop, D. (1991) *Trends Pharmacol. Sci. 12*, 383−388.

8. Sisodia, S. S., and Price, D. L. (1992) *Curr. Opin. Neurobiol. 2*, 648−652.
9. Yankner, B. A., and Mesulam, M. M. (1991) *N. Engl. J. Med. 325*, 1849−1857.
10. Esch, F. S., Keim, P. S., Beattie, E. C., Blacher, R. W., Culwell, A. R., Oltersdorf, T., McClure, D., and Ward, P. J. (1990) *Science 248*, 1122−1124.
11. Sisodia, S. S., Koo, E. H., Beyreuther, K., Unterbeck, A., and Price, D. L. (1990) *Science 248*, 492−495.
12. Kang, J., Lemaire, H. G., Unterbeck, A., Salbaum, J. M., Masters, C. L., Grzeschik, K. H., Multhaup, G., Beyreuther, K., and Muller-Hill, B. (1987) *Nature 325*, 733−736.
13. Selkoe, D. J. (1994) *Annu. Rev. Neurosci. 17*, 489−517.
14. Citron, M., Oltersdorf, T., Haass, C., McConlogue, L., Hung, A. Y., Seubert, P., Vigo-Pelfrey, C., Lieberburg, I., and Selkoe, D. J. (1992) *Nature 360*, 672−674.
15. Cai, X. D., Golde, T. E., and Younkin, S. G. (1993) *Science 259*, 514−516.
16. Golde, T. E., Cai, X. D., Shoji, M., and Younkin, S. G. (1993) *Ann. N.Y. Acad. Sci. 695*, 103−108.
17. Suzuki, N., Cheung, T. T., Cai, X. D., Odaka, A., Otvos, L., Jr., Eckman, C., Golde, T. E., and Younkin, S. G. (1994) *Science 264*, 1336−1340.
18. Felsenstein, K. M., Hunihan, L. W., and Roberts, S. B. (1994) *Nat. Genet. 6*, 251−256.
19. Games, D., Adams, D., Alessandrini, R., Barbour, R., Berthelette, P., Blackwell, C., Carr, T., Clemens, J., Donaldson, T., Gillespie, F., Guido, T., Hagopian, S., Johnson-Wood, K., Khan, K., Lee, M., Leibowitz, P., Lieberburg, I., Little, S., Masliah, E., McConlogue, L., Montoya-Zavala, M., Mucke, L., Paganini, L., and Penniman, E. (1995) *Nature 373*, 523−527.
20. Buxbaum, J. D., Oishi, M., Chen, H. I., Pinkas-Kramarski, R., Jaffe, E. A., Gandy, S. E., and Greengard, P. (1992) *Proc. Natl. Acad. Sci. U.S.A. 89*, 10075−10078.
21. Nitsch, R. M., Slack, B. E., Wurtman, R. J., and Growdon, J. H. (1992) *Science 258*, 304−307.
22. Wolf, B. A., Wertkin, A. M., Jolly, Y. C., Yasuda, R. P., Wolfe, B. B., Konrad, R. J., Manning, D., Ravi, S., Williamson, J. R., and Lee, V. M. Y. (1995) *J. Biol. Chem. 270*, 4916−4922.
23. Lee, R. K. K., Wurtman, R. J., Cox, A. J., and Nitsch, R. M. (1995) *Proc. Natl. Acad. Sci. U.S.A. 92*, 8083−8087.
24. Jolly-Tornetta, C., Gao, Z. Y., Lee, V. M., and Wolf, B. A. (1998) *J. Biol. Chem. 273*, 14015−14021.
25. Horsburgh, K., Mackay, K. B., and McCulloch, J. (1997) *Exp. Neurol. 143*, 207−218.
26. Hung, A. Y., Haass, C., Nitsch, R. M., Qiu, W. Q., Citron, M., Wurtman, R. J., Growdon, J. H., and Selkoe, D. J. (1993) *J. Biol. Chem. 268*, 22959−22962.
27. Jacobsen, J. S., Spruyt, M. A., Brown, A. M., Sahasrabudhe, S. R., Blume, A. J., Vitek, M. P., Muenkel, H. A., and Sonnenberg-Reines, J. (1994) *J. Biol. Chem. 269*, 8376−8382.
28. da Cruz e Silva, O. A. B., Iverfeldt, K., Oltersdorf, T., Sinha, S., Lieberburg, I., Ramabhadran, T. V., Suzuki, T., Sisodia, S. S., Gandy, S., and Greengard, P. (1993) *Neuroscience 57*, 873−877.
29. Hung, A. Y., and Selkoe, D. J. (1994) *EMBO J. 13*, 534−542.
30. Buxbaum, J. D., Liu, K. N., Luo, Y., Slack, J. L., Stocking, K. L., Peschon, J. J., Johnson, R. S., Castner, B. J., Cerretti, D. P., and Black, R. A. (1998) *J. Biol. Chem. 273*, 27765−27767.
31. Lammich, S., Kojro, E., Postina, R., Gilbert, S., Pfeiffer, R., Jasionowski, M., Haass, C., and Fahrenholz, F. (1999) *Proc. Natl. Acad. Sci. U.S.A. 96*, 3922−3927.
32. Arribas, J., Coodly, L., Vollmer, P., Kishimoto, T. K., Rose-John, S., and Massague, J. (1996) *J. Biol. Chem. 271*, 11376−11382.
33. Sisodia, S. S. (1992) *Proc. Natl. Acad. Sci. U.S.A. 89*, 6075−6079.
34. Haass, C., Koo, E. H., Mellon, A., Hung, A. Y., and Selkoe, D. J. (1992) *Nature 357*, 500−503.
35. Ikezu, T., Trapp, B. D., Song, K. S., Schlegel, A., Lisanti, M. P., and Okamoto, T. (1998) *J. Biol. Chem. 273*, 10485−10495.
36. Xu, H., Greengard, P., and Gandy, S. (1995) *J. Biol. Chem. 270*, 23243−23245.
37. Xu, H., Sweeney, D., Wang, R., Thinakaran, G., Lo, A. C., Sisodia, S. S., Greengard, P., and Gandy, S. (1997) *Proc. Natl. Acad. Sci. U.S.A. 94*, 3748−3752.
38. Thinakaran, G., Teplow, D. B., Siman, R., Greenberg, B., and Sisodia, S. S. (1996) *J. Biol. Chem. 271*, 9390−9397.
39. Greenfield, J. P., Tsai, J., Gouras, G. K., Hai, B., Thinakaran, G., Checler, F., Sisodia, S. S., Greengard, P., and Xu, H. (1999) *Proc. Natl. Acad. Sci. U.S.A. 96*, 742−747.
40. Chyung, A. S. C., Greenberg, B. D., Cook, D. G., Doms, R. W., and Lee, V. M. Y. (1997) *J. Cell Biol. 138*, 671−680.
41. Golde, T. E., Estus, S., Younkin, L. H., Selkoe, D. J., and Younkin, S. G. (1992) *Science 255*, 728−730.
42. Koo, E. H., and Squazzo, S. L. (1994) *J. Biol. Chem. 269*, 17386-17389.
43. Lai, A., Sisodia, S. S., and Trowbridge, I. S. (1995) *J. Biol. Chem. 270*, 3565−3573.
44. Perez, R. G., Squazzo, S. L., and Koo, E. H. (1996) *J. Biol. Chem. 271*, 9100−9107.
45. Wertkin, A. M., Turner, R. S., Pleasure, S. J., Golde, T. E., Younkin, S. G., Trojanowski, J. Q., and Lee, V. M. Y. (1993) *Proc. Natl. Acad. Sci. U.S.A. 90*, 9513−9517.
46. Pelham, H. R. (1990) *Trends Biochem. Sci. 15*, 483−486.
47. Pelham, H. R. (1991) *Cell 67*, 449−451.
48. Strous, G. J., Berger, E. G., van Kerkhof, P., Bosshart, H., Berger, B., and Geuze, H. J. (1991) *Biol. Cell 71*, 25−31.
49. Lippincott-Schwartz, J., Yuan, L., Tipper, C., Amherdt, M., Orci, L., and Klausner, R. D. (1991) *Cell 67*, 601−616.
50. Miller, S. G., Carnell, L., and Moore, H. H. (1992) *J. Cell Biol. 118*, 267−283.
51. Tomita, S., Kirino, Y., and Suzuki, T. (1998) *J. Biol. Chem. 273*, 6277−6284.
52. Sambamurti, K., Refolo, L. M., Shioi, J., Pappolla, M. A., and Robakis, N. K. (1992) *Ann. N.Y. Acad. Sci. 674*, 118−128.
53. Nishiyama, K., Trapp, B. D., Ikezu, T., Ransohoff, R. M., Tomita, T., Iwatsubo, T., Kanazawa, I., Hsiao, K. K., Lisanti, M. P., and Okamoto, T. (1999) *J. Neurosci. 19*, 6538−6548.
54. Seubert, P., Oltersdorf, T., Lee, M. G., Barbour, R., Blomquist, C., Davis, D. L., Bryant, K., Fritz, L. C., Galasko, D., Thal, L. J., et al. (1993) *Nature 361*, 260−263.
55. Turner, R. S., Suzuki, N., Chyung, A. S., Younkin, S. G., and Lee, V. M. (1996) *J. Biol. Chem. 271*, 8966−8970.
56. Buxbaum, J. D., Gandy, S. E., Cicchetti, P., Ehrlich, M. E., Czernik, A. J., Fracasso, R. P., Ramabhadran, T. V., Unterbeck, A. J., and Greengard, P. (1990) *Proc. Natl. Acad. Sci. U.S.A. 87*, 6003−6006.
57. Caporaso, G. L., Gandy, S. E., Buxbaum, J. D., Ramabhadran, T. V., and Greengard, P. (1992) *Proc. Natl. Acad. Sci. U.S.A. 89*, 3055−3059.
58. Arribas, J., and Massague, J. (1995) *J. Cell Biol. 128*, 433−441.
59. Arribas, J., Lopez-Casillas, F., and Massague, J. (1997) *J. Biol. Chem. 272*, 17160−17165.
60. Merlos-Suarez, A., Fernandez-Larrea, J., Reddy, P., Baselga, J., and Arribas, J. (1998) *J. Biol. Chem. 273*, 24955−24962.
61. Komano, H., Seeger, M., Gandy, S., Wang, G. T., Krafft, G. A., and Fuller, R. S. (1998) *J. Biol. Chem. 273*, 31648−31651.

BI001723Y